Pergamon

Journal of Structural Geology, Vol. 17, No. 3, pp. 385 to 396, 1995

0191-8141/95 $9.50+0.00

0191-8141(94)00067-0

Late brittle tectonics in a Precambrian ductile belt: evidence from brittle structures in the Singhbhum Shear Zone, eastern India

DEEPAK C. SRIVASTAVA and AKSHAYA PRADHAN

Department of Earth Sciences, University of Roorkee, Roorkee 247 667 (U. P.), India

(*Received* 10 *May* 1993; *accepted in revised form* 9 *May* 1994)

Abstract—The Singhbhum Shear Zone, a 200 km long tectonic lineament, passes close to the boundary between the Archaean 'Singhbhum craton' and the Proterozoic 'Singhbhum mobile belt'. Evidence from meso-structures reveals development of this shear zone in a ductile tectonic regime (1.6–2.2 Ga.) by thrusting of the northern block over the southern block along the N-dipping shear surface. A hitherto unrecognized, late brittle tectonic regime (≤1.6 Ga.) comprising two discrete phases is established from dynamic analysis of the fractures and veins in the shear zone. Episodic extension parallel and normal to the shear zone was a major consequence of this middle Proterozoic (≤1.6 Ga.) brittle tectonic episode, and was associated with the intrusion of a swarm of basic dykes.

INTRODUCTION

Modern structural studies on regional-scale shear zones have provided new insight into the evolution of deformed belts (Ramsay & Graham 1970, Nicolas *et al.* 1977, Coward 1980, Eeckhout & Zwart 1988, and others). Published data during the last two decades have amply demonstrated the significance of ductile shear zones in tectonics of the Precambrian shield areas (Grocott 1977, Coward 1980, Park 1981, McCourt & Vearncombe 1987). The role of the Singhbhum Shear Zone (SSZ) in geodynamic evolution of the Precambrian shield in eastern India is emphasized in this study.

The Singhbhum region records the geologic history of a period ranging from 3.4 to 1.6 Ga. Notable contributions published during the last six decades (e.g. Dunn 1929, Mukhopadhyay 1990, and Sarkar *et al.* 1992), establish 'Singhbhum' as one of the most extensively studied regions in the Indian shield. The geometry and kinematics of the 'Singhbhum Shear Zone' (SSZ), the most prominent tectonic feature in this region, however, still remains enigmatic.

GEOLOGIC FRAMEWORK OF THE EASTERN INDIAN SHIELD

The Precambrian shield in eastern India (Fig. 1) is made up of three major tectono-metamorphic belts: from north to south (i) Chotanagpur terrane (CT), (ii) Singhbhum mobile belt (SMB), and (iii) Singhbhum craton (SC). The SSZ passes close to the boundary between the SMB and the SC. It stands out as a prominent arcuate tectonic lineament extending over a length of 200 km from southeast of Mosabani in the east through Tatanagar in the central portion to Chakradharpur-Lotapahar in the west (Fig. 1).

The Chotanagpur terrane consists of repeatedly deformed and polymetamorphosed migmatitic gneisses, charnockites, granulites, mafic-ultramafic rocks and metasediments. Structural and stratigraphic relationships amongst the different lithotectonic units in the CT are not as yet understood. The SMB comprises the early Proterozoic (2.3–2.4 Ga.) fold belts consisting of thick volcanics and interbedded greenschist to amphibolite facies metasediments. The Singhbhum craton is made up of a huge granitic batholith (the Singhbhum granite 3.1–3.3 Ga.) and the enveloping Iron Ore Group metasediments (> 3.1 Ga.; Saha *et al.* 1988). Numerous but conflicting stratigraphic successions have been proposed for the Precambrian shield of eastern India (Mukhopadhyay 1990). As the details of stratigraphic controversies are beyond the scope of this paper, we present a simplified stratigraphic succession to outline the relative geochronologic positions of the major rock groups belonging to the 'SMB' and the 'SC' (Table 1).

TECTONIC FRAMEWORK OF THE SSZ AND THE SCOPE OF THIS STUDY

According to Dunn (1929), Dunn & Dey (1942) and Sarkar & Saha (1962, 1977), the major structure in the Proterozoic SMB is an anticline ('Singhbhum anticlinorium') on an E–W trending axial-surface. They interpreted the southern limb of this anticline as overturned and thrust against the Archaean craton (SC) along the 'Copper belt thrust' (synonymous to SSZ). Furthermore, according to Sarkar *et al.* (1969) and Sarkar & Saha (1977), the SSZ demarcates the boundary between the Proterozoic (SMB) and the Archaean (SC) orogenic belts. On the basis of normal stratigraphic sequences in some sectors, Mukhopadhyay (1976) questioned this interpretation regarding overturning and the

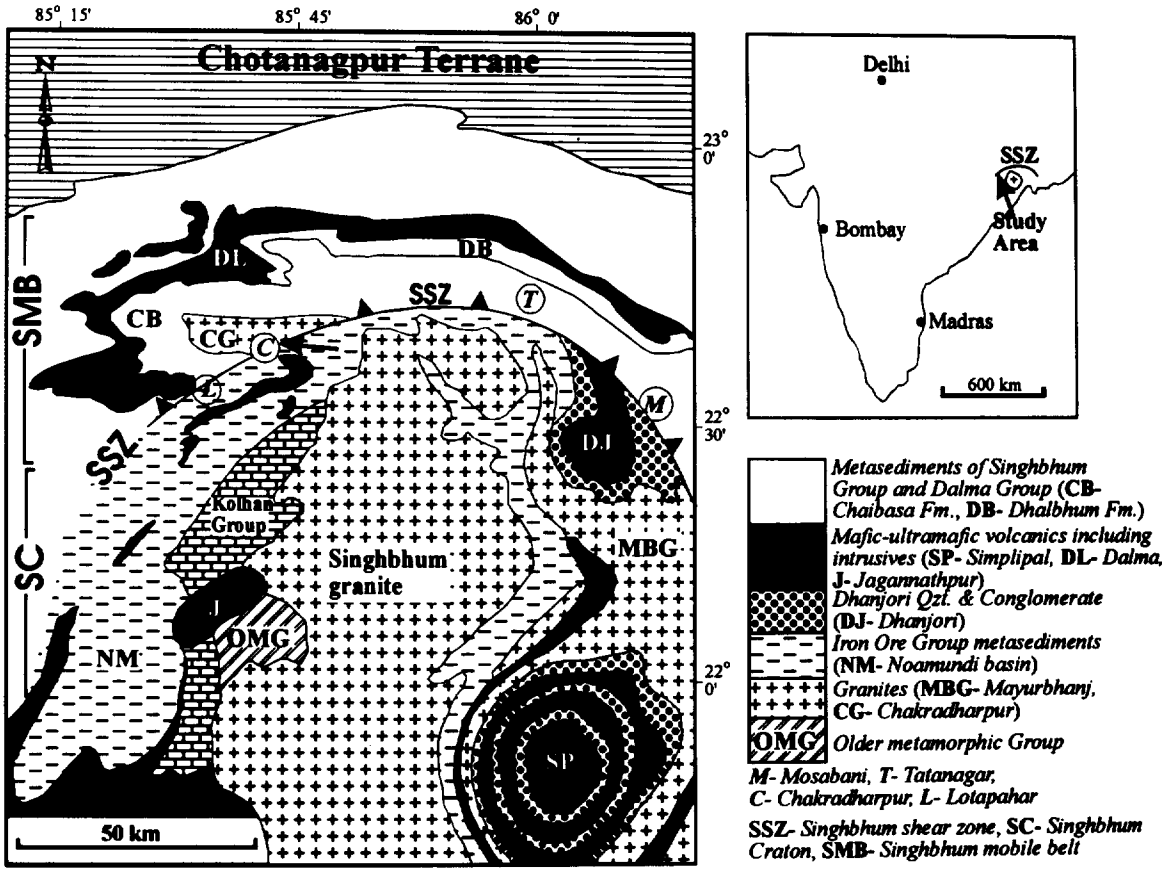

Fig. 1. Geological map of Singhbhum region (simplified after Dunn 1929, Dunn & Dey 1942, Sarkar & Saha 1977: arrow shows location of the study area). Inset shows location of Singhbhum Shear Zone (SSZ) in India.

Table 1. An outline of the simplified stratigraphy of the Singhbhum craton (**SC**) and the Singhbhum mobile belt (**SMB**). (Slightly modified after Sarkar 1982, Sarkar & Saha 1983 and Saha *et al.* 1988)

AGE (Ga.)	South of Singhbhum shear zone			North of Singhbhum shear zone	
1.6–0.95	Newer dolerite dykes and sills				
2.1	Mayurbhanj granite Gabbro–anorthosite Ultramafic intrusions				
2.2–2.1	Conglomerate, Sst., Lst. and Shales—	KOLHAN GROUP		Soda granite, Arkasani granophyre	
2.3	Dhanjori volcanics (Simlipal/Jagannathpur volcanics)	DHANJORI GROUP		Upper Dalma Formation (Dalma volcanics) Lower Dalma Formation (Mafic–ultramafic tuffs, phyllites, Ironstones and Lst.)	DALMA GROUP
2.4–2.3	Dhanjori metasediments = Ongarbira volcano-sedimentary belt		*MOBILE BELT*		
				Dhalbhum Formation (Phyllite, schist and quartzites) Chaibasa Formation (Mica-schist and quartzites with metabasics)	SINGHBHUM GROUP
		UNCONFORMITY			
3.1	Singhbhum granite (late phase) Epidiorites			Chakradharpur granite gneiss	
SINGHBHUM CRATON	Upp. Shale, Sst. and volcanics Banded Iron Formations Lr. Shale, tuffs and acid volcanics Mafic lavas and tuffs Sandstones and conglomerates	IRON ORE GROUP			
		UNCONFORMITY			
3.3	Singhbhum granite (early phase)				
3.4	Older metamorphic tonalite gneiss Older metamorphic supracrustals—	OLDER METAMORPHIC GROUP			

consequent thrusting of the southern limb of the 'Singhbhum anticlinorium'. Mukhopadhyay *et al.* (1975) and Mukhopadhyay (1976) further contended that the SSZ is not a thrust but a zone of 'intense flattening' or 'compression'. Ghosh & Sengupta (1987), for the first time, reported the occurrence of small-scale ductile shear zones from Surda (near Mosabani in Fig. 1), implying that the SSZ may represent a large scale ductile shear zone.

Considerable work on the structural geometry in different parts of the SMB and the SC has already been completed (e.g. Bhattacharyya & Sanyal 1988, Sarkar & Saha 1983). The SSZ, itself, however, has not been investigated in detail except for a few accounts on the meso-folds in its eastern and central parts (Mukhopadhyay *et al.* 1975 and Ghosh & Sengupta 1987). Despite a general consensus that the SSZ is a zone of high strain, neither its kinematics (e.g. normal/strike-slip/thrust) nor the mechanism of its development is understood. We attempt to address some of these outstanding questions by analyzing the brittle and ductile structures in the western extremity of the SSZ around Chakradharpur (Fig. 1). For the first time, we report and evaluate the kinematic significance of the brittle structures within the SSZ.

LITHO-STRATIGRAPHY OF THE SSZ

The SSZ is a zone of northerly dipping, *L–S* mylonites hosting rich deposits of copper, uranium and apatite–magnetite. Due to its lensoid nature, the thickness of shear zone varies from a couple of hundred metres near its eastern and western extremities to over 3 km in the central part near Tatanagar (Fig. 1). Whereas the northern boundary of SSZ is gradational with the Singhbhum Group metasediments (2.4–2.3 Ga., Table 1), its southern boundary is defined by sharp contacts between the shear zone mylonites and rocks of diverse litho-stratigraphy in different sectors (Sarkar *et al.* 1992).

In the eastern sector near Mosabani (Fig. 1), the shear zone rocks (deformed amygdaloidal basalts, chlorite–biotite schist, feldspathic schist, impersistent bands of conglomerate and kyanite-bearing quartzites) overlie the Dhanjori Group of rocks (2.4 Ga.). In the central sector near Tatanagar, the SSZ mylonites (quartz–chlorite schist, quartzite and quartzo–feldspathic schist) overlie pelites above the Singhbhum granite (3.1–3.3 Ga.). Whether these pelites belong to Dhanjori Group (2.4 Ga.) or Iron Ore Group (c. >3.1 Ga.) is still controversial. In the western sector near Chakradharpur (Fig. 1), the SSZ comprises a suite of mylonitized rocks (ferruginous-orthoquartzites, slates/phyllites, dolostones, conglomerates, quartzo–feldspathic schist) resting above the low-grade Iron Ore Group metasediments (>3.1 Ga., Saha *et al.* 1988). Within the SSZ, several small bodies of sheared sodic granites and granophyres occur in different parts. Some of these granites represent basement slices (>3.1 Ga., Mukhopadhyay *et al.* 1980) and others mark a 2.2 Ga. event of acidic intrusion (Saha *et al.* 1986).

In summary, the SSZ cuts through Precambrian rocks ranging in age from older than 3.1 Ga. (Iron Ore Group, basement slices etc.) to 2.2 Ga. (Singhbhum Group, soda-granites etc.). As discussed later, the SSZ does not affect 1.6 Ga. old 'Newer dolerite' dykes. These constraints imply that the development of the SSZ took place between 1.6 and 2.2 Ga.

STRUCTURES IN THE WESTERN PART OF SSZ

Large scale structure

Within the study area, the SSZ is represented by a 100–200 m thick sequence of alternating slate-phyllite and dolostone bands of metre-scale thickness. This sequence is repeated structurally several times as a consequence of large scale, NE-plunging isoclinal folding. Due to intense shearing, the slates and phyllites have been converted into phyllonites and the dolostones are mostly mylonitized. Polyphase ductile and brittle structures, developed profusely in these rocks, offer an opportunity for detailed structural analysis of the shear zone.

Meso-structures

Folds. Folds of four successive phases are well preserved in the shear zone rocks. The earliest folds (F_{1A}) are typically close to tight and intrafolial folds traced by sedimentary layering (S_0) and bedding-parallel quartz veins. F_{1A} axial planes and limbs are co-axially refolded by another set of tight to isoclinal folds (F_1) resulting in type-3 interference patterns (Ramsay 1967). On account of identical geometry and orientation, both F_{1A} and F_1 folds are grouped within the first phase of deformation in this study (Fig. 2a).

The geometry of F_1 folds is controlled largely by the extent of shearing. Thus, the F_1 folds are reclined only when they are caught up in the zones of intense shearing. With decrease in the amount of shearing, the plunge of F_1 axes become shallow and the folds assume 'inclined-plunging' geometry. The orientation of the axial plane foliations (S_1), however, does not vary with the amount of shearing because these foliations were oriented parallel to the shear surfaces during the course of ductile shearing. Evidently, the effect of shearing was restricted to the rotation (steepening) of the F_1 axes within axial planes of relatively consistent orientation.

Structures of the first phase are overprinted by a set of open to close and doubly plunging F_2 folds showing conspicuous axial planar fanning of the E–W striking and steeply dipping crenulation foliation 'S_2' (Fig. 2b). Within the SSZ, the third phase of deformation is represented by open to gentle F_3 folds on *N–S* striking and steeply dipping axial planes 'S_3' (Fig. 2c). The F_3 axial planes are perpendicular to both F_1 and F_2 axial planes and, the F_3 axes plunge 30–50° towards NNE (Fig. 2c). Except for a few discrete fractures, no pene-

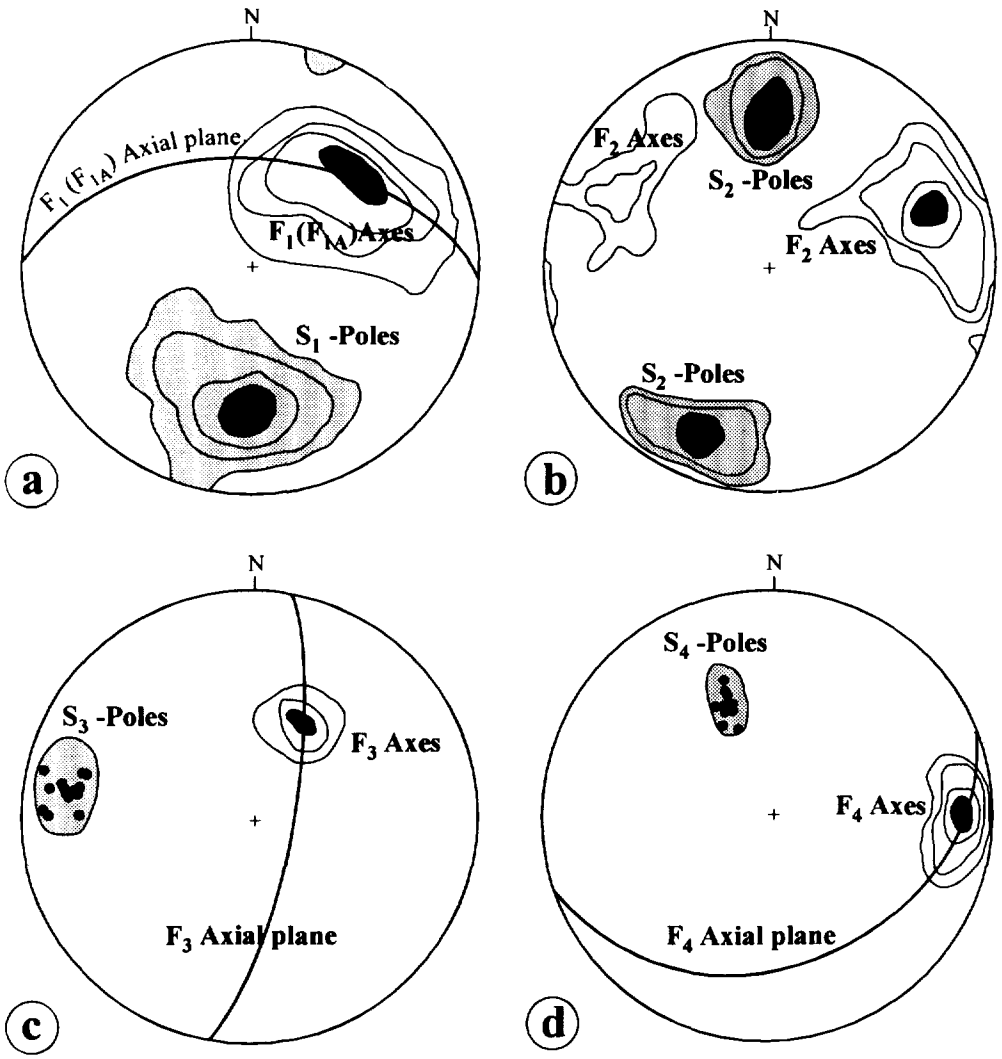

Fig. 2. Equal area stereo-plots of axial planes and axes. Contour % per 1% area, (a) 1–2–6–12% for axial plane foliation (S_1) and 1–3–8–15% for axes. Total 219 axial planes and 156 axes of F_1 and F_{1A} folds, (b) 3–5–13% for axial planes (S_2) and 1–2–8–13% for axes. Total 39 axial planes and 142 axes of F_2 folds, (c) 6–46–60% for axes. Total 14 axial planes and 35 axes of F_3 folds, (d) 1–6–40–49% for axes. Total 10 axial planes and 71 axes of F_4 folds.

trative axial plane foliation developed during the F_3 phase of deformation.

Kink bands on sub-horizontal axial planes represent the last phase of the folding (F_4) in the shear zone rocks. Mukhopadhyay *et al.* (1975), Sarkar & Srivastava (1982) and others have grouped these structures together with the F_2 structures due to their low axial-plunges and approximately E–W strike of the axial planes. We consider F_2 folds different from F_4 folds as the former are characterised by plane-non-cylindrical geometry and steep crenulation foliations parallel to the axial plane (Figs. 2b & d).

Shear zones. Meso-scale ductile shear zones with distinct *S* and *C* structures (Berthé *et al.* 1979) are exceptionally well developed in phyllonites of the SSZ (Fig. 3a). Consistency in orientation and geometry of meso-shear zones imply their synchronous development. That the deformation leading to the development of meso-shear zones is correlatable to the evolution of the macroscopic SSZ is revealed by the parallelism between *C*-surfaces (*e–w* strike and N-dip) and the generalized orientation of the SSZ. Two lines of evidence from the *X–Z* sections of meso-shear zones (Fig. 3a, looking towards east) reveal that the SSZ is a thrust zone. First, the sense of asymmetry of the sigmoidal pods (*S*-shaped) implies up-dip movement on the N-dipping shear planes (*C*-surfaces). Second, the acute angle relationships between *S*- and *C*-surfaces imply a consistent 'top to the south' movement along the N-dipping shear surfaces.

Effect of shearing on F_1 *folds.* Within the individual shear zones, the F_1 folds are predominantly reclined and sometimes plane-non-cylindrical resembling sheath-like geometries. Sheath-folding in the SSZ is further corroborated by the elliptical outcrop patterns in mylonitic quartzite underlying the dolostone-phyllite sequence (complex interference patterns of Srivastava & Sarkar 1985). On account of very acute apical angles (15–25°) in these sheath-folds, the fold hinges are parallel to *X*-direction (NE) except at sharp bends. It is, therefore, likely that many of the apparently cylindrical and reclined folds in the SSZ are actually the steep segments of

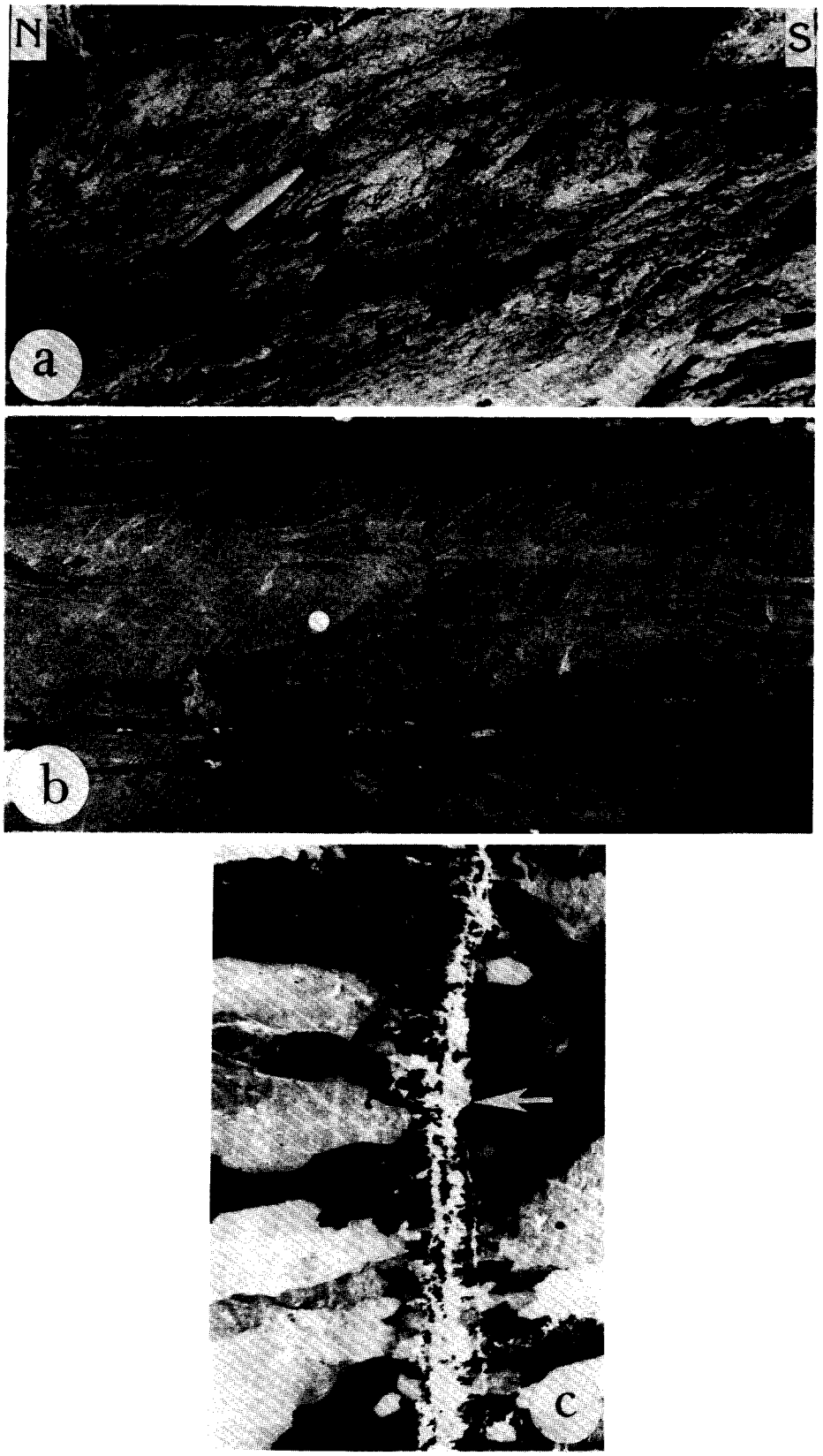

Fig. 3. (a) Ductile shear zones in phyllonite (X–Z section, looking towards east). Pen cap 6.5 cm. (b) S-type plumose structure with parabolic arrest lines. Diameter of coin 2.4 cm. (c) Wall rock inclusion band (indicated by arrow) in the central portion of a quartz-filled transverse vein (cross-polars, negative print). Field of view 2.2 cm × 1.4 cm.

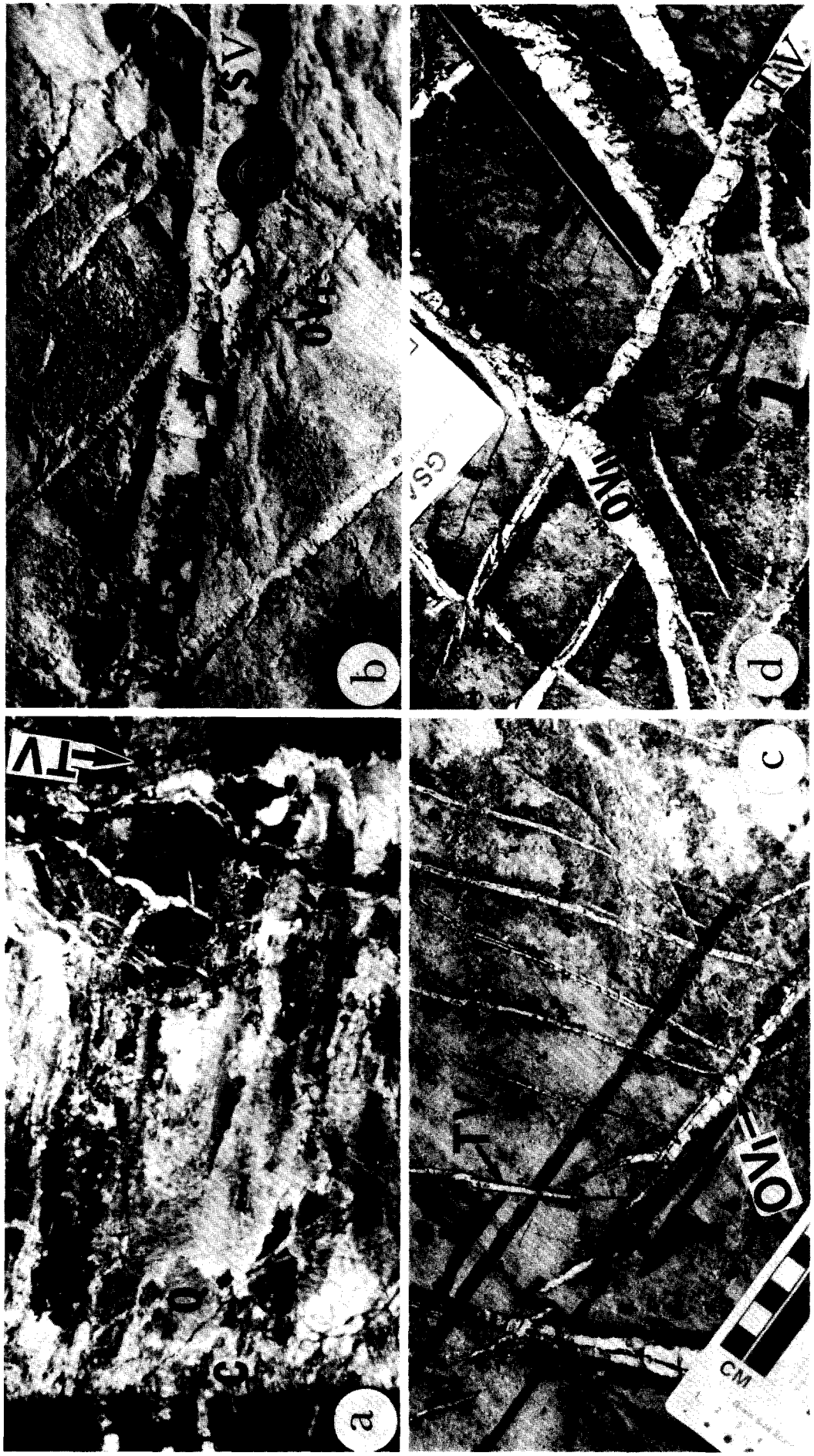

Fig. 4. (a) Oblique vein (OV_{II}) cutting a thin transverse vein (TV—indicated by arrow). OV_{II} is a composite vein with calcite fibres (C) at the margin and quartz fibres (Q) in the median portion. Both in OV_{II} and TV, the fibres are perpendicular to vein boundaries (cross-polars). Field of view 14.5 mm × 10 mm. (b) Strike Vein (SV) cutting oblique veins (OV_I) with small amount of apparent right-lateral offset due to dilation. Vein fill in SV and OV_I is made of coarse-blocky and fibrous quartz, respectively. Diam. of coin 2.4 cm. (c) & (d) Inconsistent cross-cutting relationships. In (c), OV_I cuts through TV except in the upper left part where a thick TV cuts OV_I. OV_I shows branching and en échelon tip veins. In (d), TV cuts OV_{II} in the lower right corner and OV_{II} cuts TV in the central portion of the Fig. Pen length 11 cm.

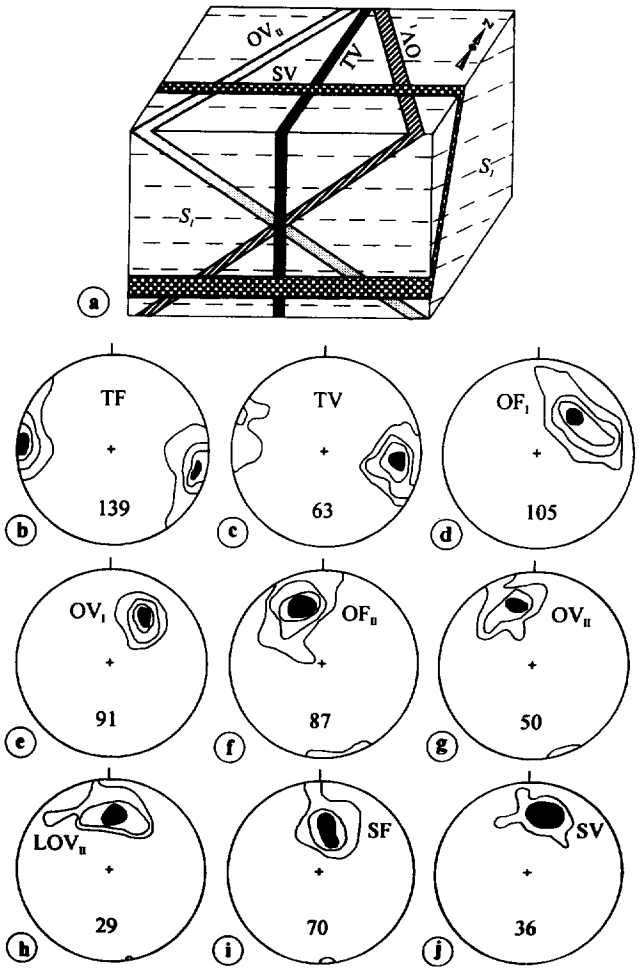

Fig. 5. (a) Schematic diagram showing the classification scheme for the brittle structures (TV—transverse vein, OV_I and OV_{II}—oblique veins, SV—strike vein, S_I—regional foliation in SSZ). Same classification holds good for the fractures. (b)–(j) Equal area stereo-plots of fractures and veins. Contour % per 1% area; (b) 1–5–11–15%, (c) 1–5–10–20%, (d) 1–4–9–15%, (e) 1–12–25–40%, (f) 1–7–11–17%, (g) 2–10–32%, (h) 3–10–18%, (i) 1–10–18%, (j) 3–25%. Number in each stereogram represents total data (TF—Transverse fracture, OF_I and OF_{II}—Oblique fractures, SF—Strike fracture, LOV_{II}—Late oblique vein of second set).

sheath folds. The present orientations of F_1 axes have been achieved after their rotation into parallelism with the X-direction during progressive shear. Similar rotations of the fold axes towards the X-direction have been demonstrated by Ghosh & Sengupta (1987) in the eastern part of the SSZ.

Effect of shearing on F_2 *folds.* The progressive increase in the abundance of F_2 structures towards the SSZ (Sarkar & Srivastava 1982) suggests that the F_2 structures are related to the shearing event. Furthermore, the non-cylindrical geometries of the F_2 folds are result of the rotation of F_2 axes during the course of progressive shearing. In comparable lithologies, the F_1 axes are much more acutely curved than the F_2 axes implying that the F_1 folds were modified by higher amounts of shear as compared to the F_2 folds.

Time relationship between folding and shearing. Unlike the first two sets of folds (F_1 and F_2), neither the F_3 and F_4 folds nor the subsequent brittle structures show any imprint of shearing. The shearing, therefore, must have ended prior to the development of F_3 structures. In contrast, the earliest structure that can be related to the shearing is the mylonitic foliation parallel to F_1 axial planes. Based on these arguments, we infer that the development of SSZ started with intense shearing during or shortly after the F_1 folding and it continued until the end of F_2 folding with declining amount of shear. By the time the F_3 folds started developing, the SSZ had already evolved in the eastern Indian Precambrian shield.

BRITTLE STRUCTURES

Four sets of brittle fractures and corresponding veins are distinguished in the shear zone rocks (Fig. 5a). On the basis of their angular relationship with the strike of the dominant foliation (S_1), these structures can be classified as: (i) transverse fractures (TF) and transverse veins (TV) with strikes normal to the strike of S_1, (ii) strike fractures (SF) and strike veins (SV) with strikes parallel to the strike of S_1, (iii) first set of oblique fractures (OF_I) and oblique veins (OV_I) and (iv) second set of oblique fractures (OF_{II}) and oblique veins (OV_{II}).

Classification scheme and the orientations of these four sets of brittle structures are shown in Figs. 5(a) & 5(b)–(j), respectively.

Within the SSZ, barren fractures are observed in phyllonites whereas quartz veins are restricted to dolostones. Most likely, in dolostones, the syntectonic fluids dissolved silica (chert) and deposited it as quartz in nearby fractures to form veins. In phyllonites, the fractures remained barren due to the absence of such readily soluble silica.

Fractures

Three lines of evidence suggest a predominantly extensional mode of origin for all the fracture sets in the SSZ. These are: (i) lack of shear offset in most of the cross-cutting fractures, (ii) termination of fractures at the bedding plane boundaries, and (iii) plumose architecture of the fracture-surfaces (Fig. 3b). Commonly, the plumose structures are *S*-type (Bahat & Engelder 1984) and break into twist hackles near the bedding plane boundaries due to sudden changes in stress orientations. The presence of fringe zones with twist hackles reveals the hybrid (shear/extension) nature of some of these fractures (particularly OF_I and OF_{II}). Furthermore, the parabolic shapes of plumose structures suggest that the magnitudes of both the fracturing stress and fracturing velocity were maximum along the plume axis and declined gradually towards either end (Kulander & Dean 1985).

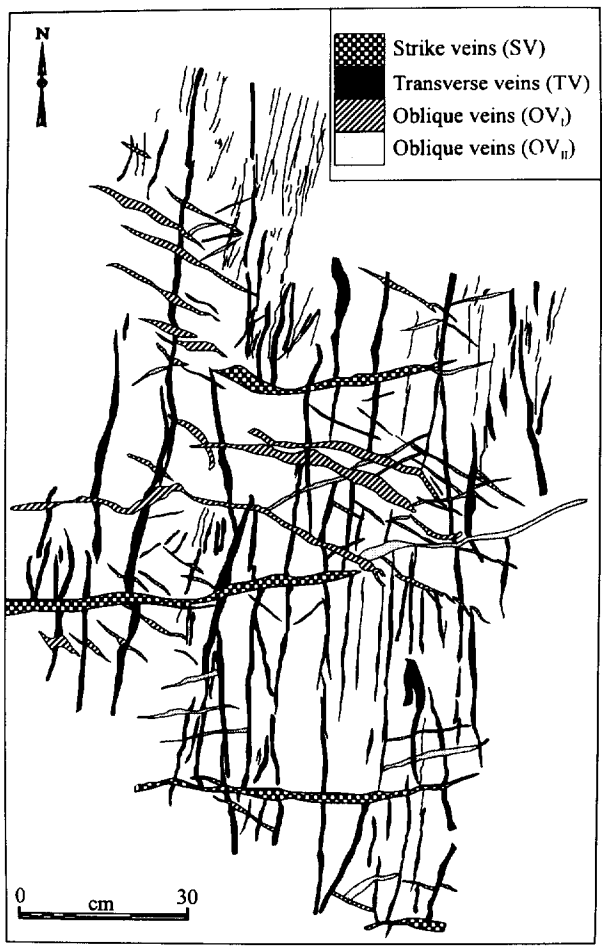

Fig. 6. Map showing inconsistent cross-cutting relationships amongst different sets of veins.

Veins

Veins belonging to four different sets (TV, OV_I, OV_{II} and SV) produce complex patterns (Fig. 6) on almost every outcrop of dolostone in the SSZ. Within a set of sub-parallel veins of variable dimensions, the most prominent and straight veins are termed 'master veins' and the arrays of thin en échelon veins near tips of the master veins are referred as 'tip-veins' (Figs. 4c and 6). Quartz constituting more than 95% (by volume) of the vein infillings occurs as fine and coarse fibres in TV, OV_I and OV_{II} (Figs. 3c and 4a) and as milky-white blocky crystals in SV. Calcite, forming only a minor component (<5%) of the vein infillings, occurs as fine fibres along the marginal parts in multimineralic and 'composite' veins (Fig. 4a, cf. Ramsay & Huber 1983).

Vein structure. Wall-rock inclusion bands (Fig. 3c), inclusion trails, matching vein-wall boundaries, vein normal fibres (Fig. 4a) and common lack of shear offsets (Fig. 6) suggest that most veins evolved by a crack-seal mechanism through extension fracturing (mode-I). In veins with sigmoidal fibres, the angle between vein-margin and fibre decreases systematically from 90° in the median region to ≤70° in the marginal portion implying an antitaxial growth (Durney & Ramsay 1972, p. 72). An implication of antitaxial growth is that the coarse fibres and the blocky quartz crystals occurring in the median portions of the veins are paragenetically older than the fine quartz fibres along the marginal parts. In rare 'composite-veins', the oldest fracture was sealed by syntaxial growth of calcite fibres occurring now along both the margins (Fig. 4a). The subsequent cracks developed through the calcite infilling were sealed by successive growths of coarse and fine quartz fibres in an antitaxial sense. SV are rarely fibrous and most of them consist only of milky-white and blocky quartz crystals.

Transverse veins (TV). N–NNE striking and steeply dipping TV are developed only as master veins (1 mm–2 cm thick and few metres long) and do not form en échelon arrays. These veins show clear geometric evidence, such as fibres perpendicular to vein walls and lack of significant shear offset, in favour of their extensional origin (Figs. 4a and 6).

Oblique veins (OV_I and OV_{II}). Both the master and the tip veins in these sets occur commonly in en échelon arrays (Figs. 4b & c and 6). Some of the large and sigmoidal OV_{II} veins are cut by small lenticular veins (LOV_{II}) oriented parallel to the tips of the sigmoids. These LOV_{II} veins must have developed during the late stages of shearing when the sigmoidal OV_{II} veins had attained their limits of rotation (Durney & Ramsay 1972, p. 85). Another characteristic of oblique veins is the forking and branching near the terminations (Fig.

4c). Whereas the forking is a consequence of unstable fracture propagation and dissipation of excess kinetic energy near the tips, the branching implies oblique relationships between these veins and the principal planes of stress (Bieniawski 1967). As the oblique veins show both the characteristics of extensional (vein normal fibres, Figs. 4a & b) as well as shear (small amounts of lateral offsets) origin they must have developed by hybrid mode (shear/extension) of fracturing.

Strike veins (SV). This set, consisting of E–W striking and southerly dipping master veins, differs from all other vein sets (TV, OV_I and OV_{II}) in three respects. First, the SV invariably cross-cut all other veins (Figs. 4b and 6). Second, they are the thickest (1.5–4 cm) and continue for several tens of metres. Third, the vein fill in SV is made up of coarse, milky and blocky quartz (Fig. 4b) in contrast to the grey and fibrous quartz in all other vein-sets. While cross-cutting, the SV dilationally pull apart the older veins to suggest their origin by extension fracturing (Fig. 6). Some of the SV, however, are oriented sub-parallel to the OV_{II}/LOV_{II} veins (Figs. 5g–j), but in all such cases, the distinction between these two types of veins can be made on the basis of the texture of vein fill (fibrous or blocky quartz), dimension of vein and cross-cutting relationship.

Sequence of vein development

A total of 203 distinct cross-cutting relationships amongst different veins were studied on outcrops and confirmed by microscopic studies on critical thin sections. These observations reveal a complex and ambiguous order of overprinting amongst the two sets of oblique veins (OV_I and OV_{II}) and TV. Three types of vein sequences are most common. First, on a given outcrop, a particular TV cuts one OV_{II} vein and within a few cm, is itself cut by another OV_{II} vein (Fig. 4d, also see Fig. 6). Second, inverse cross-cutting relationships between TV and OV_{II} veins are observed on different outcrops. Third, some vein intersections imply a synchronous relationship as the two veins run into each other and neither of the veins cuts the other vein. These three types of relationships are commonly observed between the TV and OV_I veins (Fig. 4c) as well as between the OV_I and OV_{II} veins. SV, marking the last phase of brittle deformation in the area, cut through all other veins invariably (Figs. 4b and 6).

In summary, the overprinting relationships amongst different vein-sets in the SSZ establish two distinct phases of brittle tectonics (BT_1 and BT_2). Whereas the transverse (TV and TF) and oblique (OV_I, OV_{II}, OF_I and OF_{II}) structures were developed during the early phase (BT_1), the development of SV and SF took place during the late phase (BT_2).

STRESS ORIENTATIONS

The mode of fracturing in brittle tectonics is controlled largely by the amount of effective differential stress ($\sigma_1'-\sigma_3'$) in relation to the tensile strength (T) of the rock. Extension and shear fractures develop at $\sigma_1'-\sigma_3' \leq 4T$ or $\sigma_1'-\sigma_3' \geq 8T$, respectively. If, however, the effective differential stress assumes different values between 4T and 8T in a single deformation, a spectrum of dynamically compatible and co-axial 'hybrid-fractures' is developed ('joint spectra' in Hancock 1986). Thus in order to determine the orientations of the principal stress axes, different principles have to be applied for the different modes of fractures. For example, the extension fractures (such as TF/TV or SF/SV in the SSZ) develop parallel to the $\sigma_1-\sigma_2$ plane and normal to the σ_3 axis. Conjugate shear fractures yield principal axes according to Anderson's law (Anderson 1951). The hybrid fractures (such as oblique fractures and veins in the SSZ) enclosing a dihedral angle of $<60°$ intersect along the σ_2 axis. In such hybrid fractures, the orientations of σ_1 and σ_3 axes are given by acute and obtuse bisectors of the dihedral angle, respectively.

Stress analysis of the transverse and oblique structures reveals two different orientations of the principal stress axes in the BT_1 phase. Extensional origin of the transverse structures suggests an east–west directed, subhorizontal σ_3 axis and a N–S striking subvertical $\sigma_1-\sigma_2$ plane (Figs. 7a & b). In contrast, due to their hybrid mode of origin, the oblique structures reveal an east–west directed and subhorizontal σ_1 axis, S–SSW trending σ_2 axis and N–NNE trending σ_3 axis (Figs. 7c & d). Thus despite the fact that transverse and oblique structures are considered to be broadly coeval on the basis of cross-cutting relationships, they were produced not only at different amounts of the effective differential stress but also under different orientations of principal stress axes.

The second phase of brittle tectonics (BT_2) was rather simple and resulted in development of pure extensional types of SF and SV in a stress configuration defined by a northerly directed σ_3 axis and an E–W striking but southerly dipping $\sigma_1-\sigma_2$ principal plane (Figs. 7e & f). Independent evidence to constrain the orientations of σ_1 and σ_2 axes during the development of SV is lacking. As the SV consistently cut through the other veins on all scales, the local and regional stress conditions were consistent with each other during their development. Furthermore, as these structures are thickest and most extensive, this phase must have resulted in considerable extension normal to the belt (σ_3 in N–S direction).

The field evidence of inconsistent cross-cutting relationships amongst TV, OV_I and OV_{II} veins can be best explained by episodic growth of these structures during the BT_1 phase. Such a growth must have been accomplished by changes in both the effective differential stress and the orientation of the principal stress axes. For example, TV must have developed at low amounts of differential stress and with the σ_3 axis oriented E–W. Due to quick rotation of the σ_3 axis to a north–south direction and increase in differential stress, oblique veins started developing at the expense of TV. Depending upon whether the σ_3 axis was oriented E–W or N–S and whether the effective differential stress was $<4T$ or between 4T and 8T during the subsequent event, the

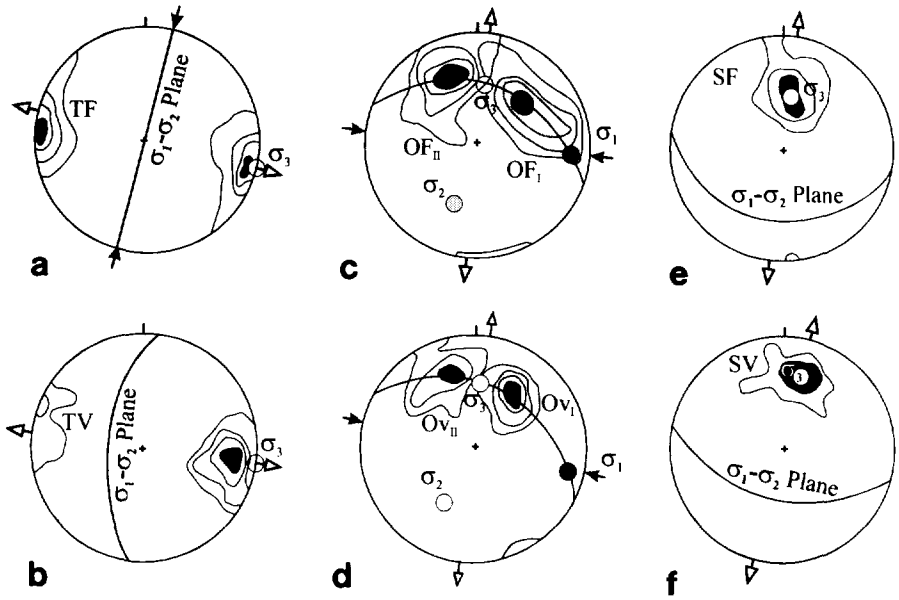

Fig. 7. Equal area stereo-plots showing results of stress analysis from extensional type of transverse structures (in a & b), hybrid type of oblique structures (in c & d) and extensional type of strike-parallel structures (in e & f). Blank and outward directed arrows—direction of maximum extension (σ_3); black & inward arrows—direction of maximum compression (σ_1). Contour %, number of data and abbreviations as in Figs. 5(b)–(j).

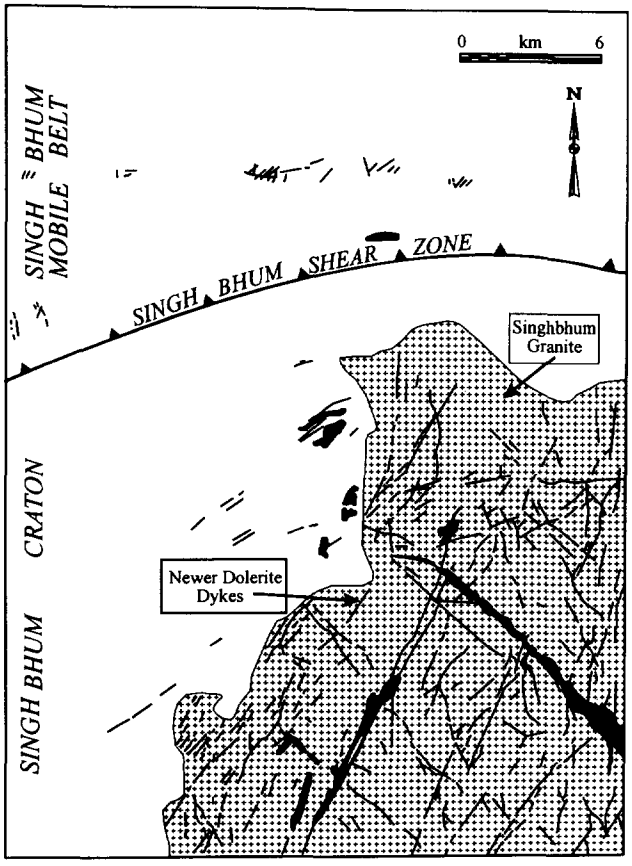

Fig. 8. Geological map (after Dunn 1929) showing the orientation of the 'Newer dolerite' dykes (unornamented areas—metasediments including volcanics and associated rocks). Note that the orientations of dykes are not affected by the Singhbhum Shear Zone.

respective development of TV or oblique veins took place.

DISCUSSION

Significance of small scale structures

The SSZ records a history of four phases of folding, ductile shearing and two phases of brittle fracturing. In the chronology of small scale structures, the relative age of the SSZ ranges from syn- to post-F_1 folding to the F_2-folding. F_3 and F_4 folds, brittle fractures and veins all developed subsequent to the evolution of the SSZ by thrusting of the northern block over the southern block on shear planes dipping towards the mobile belt on the north. Our work supports the interpretations of Dunn & Dey (1942) and Sarkar & Saha (1977) that the SSZ is a 'thrust', at least in kinematic sense (Ghosh & Sengupta 1990). Furthermore, the asymmetry of meso-structures (Choukroune *et al.* 1987) implies that the SSZ is not merely a zone of 'intense flattening' (Mukhopadhyay *et al.* 1975, Mukhopadhyay 1976), but also a zone of high strains developed predominantly by simple shear with or without the combination of pure shear. It is evident that during the development of the SSZ, crustal thickening must have taken place due to shearing on low to moderate dipping planes.

Predominantly antitaxial and crack-seal type of syntectonic veins, developed during the brittle regime, evolved through filling of fractures by locally derived and freely circulating fluids in dolostone bands. As these veins and fractures are not affected by folding movements and they cut through all the compressive ductile structures, the brittle tectonics post-dates the evolution of folds and shear zones. Episodic extensions parallel

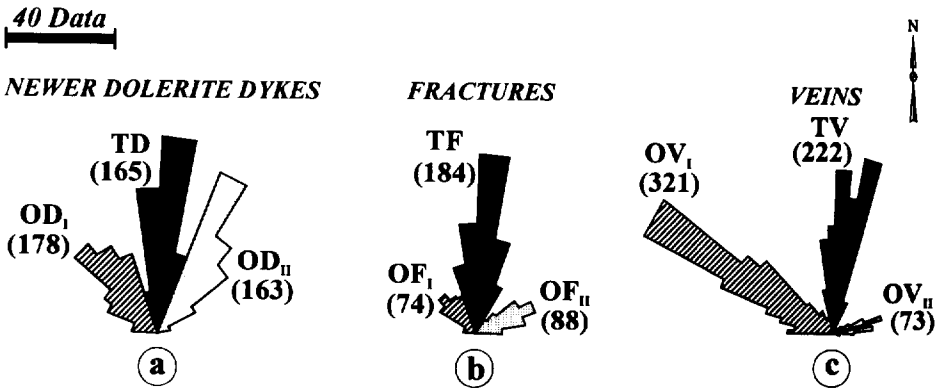

Fig. 9. Rose diagrams showing orientations of (a) 'Newer dolerite' dykes, (b) fractures and (c) veins. TD—Transverse dykes, OD_I and OD_{II}—two sets of oblique dykes. Data in (a) has been measured from Fig. 8.

and normal to the SSZ were major consequences of the brittle deformations.

Our work shows that the inconsistent cross-cutting relationships amongst different sets of brittle fractures/veins reflect the heterogeneous stress conditions that can be classified into two (or more) events of homogeneous stress conditions by a careful study of fracture/vein geometry and their dynamic analysis.

Regional implications

Intrusion of 'Newer dolerite' dykes extending up to several tens of km (Fig. 8), mark the youngest event in the tectono-stratigraphy of Singhbhum craton (Table 1; Dunn 1929, Dunn & Dey 1942, Sarkar & Saha 1977). Dunn (1929) presented unambiguous evidence of these dykes cutting across the rocks of varied ages (Singhbhum granite 3.1–3.3 Ga., Dalma epidiorite 2.3 Ga., Arkasani granophyre 2.2 Ga.). Available K/Ar age data on the 'Newer dolerite' dykes (1.6–0.9 Ga., Sarkar & Saha 1977) suggest that c. 1.6 Ga. is the age of intrusion of these dykes and the younger ages reflect the probable effects of metamorphism.

We argue for a synchronous relationship between the 'Newer dolerite' dykes and the brittle structures (veins and fractures) discussed in this paper for two reasons. First, both sets of structures share a common mechanism of development by predominant extensional fracturing (Dunn 1929). Second, the orientations of the dykes shown on Dunn's (1929) map fall in three prominent sets (TD, OD_I and OD_{II}) matching closely with the orientations of the three sets of fractures (TF, OF_I and OF_{II}) and veins (TV, OV_I and OV_{II}) in the SSZ (Figs. 9a–c). On the basis of these genetic and geometric correlations, we infer that the brittle tectonics post-dating the development of SSZ is about 1.6 Ga. old.

Several conflicting models have been proposed for the geodynamic evolution of the Precambrian shield in eastern India, e.g. intraplate subduction (Sarkar & Saha 1977), back-arc marginal basin (Bose & Chakraborty 1981), ensialic rifting (Gupta *et al.* 1980), microcontinental collision (Sarkar 1982) and tectonic underplating (Mukhopadhyay 1990). Of these, Mukhopadhyay's (1990) model ascribing the development of SSZ to the delamination and sinking of the subcrustal lithosphere during a compressional tectonic regime is most favoured.

Our interpretations are different from these models in the sense that we identify two phases of brittle tectonics (BT_1 and BT_2) subsequent to the development of the SSZ. Implicit in some of these existing models is the necessity to assume the intrusion of 'Newer dolerite' dykes prior to the development of SSZ. Such an assumption contradicts the field evidence showing the intrusions of 'Newer dolerite' dykes in the Dalma epidiorites (Dunn 1929, pp. 134–135; Table 1). Furthermore, if the dykes are older than shearing then why has the SSZ not affected the orientation of these dykes significantly (even in those areas where these two are spatially very close to each other, e.g. northern border of the Singhbhum granite, Fig. 8)? We, therefore, conclude that the dykes, fractures and veins developed in the SSZ and adjoining areas represent a brittle regime of deformation subsequent to the evolution of the SSZ. Such a conclusion is consistent with the field evidence, structural relationships, regional stratigraphy (Saha *et al.* 1988), and the stress orientations revealed by the dynamic analysis of the brittle fractures and veins.

CONCLUSIONS

Two major geo-tectonic regimes of contrasting styles affected the evolution of eastern Indian Precambrian shield subsequent to the evolution of the Proterozoic mobile belt (SMB). During the older and ductile regime (c. >1.6–2.2 Ga.), intense horizontal shortening in a north–south direction gave rise to the development of SSZ by thrusting of the northern block (predominantly Singhbhum mobile belt) over the southern block (predominantly Singhbhum craton). This ductile regime represents relatively deep crustal deformation and resulted in crustal thickening during the early Proterozoic Period.

In the middle Proterozoic Period (c. $\leq$ 1.6 Ga.), the pre-existing ductile structures were superimposed by brittle structures formed at shallower crustal level. This middle Proterozoic brittle deformation, characterized

by the fluctuations in effective differential stress and the orientations of principal stress axes, resulted in episodic extensions parallel and normal to the major tectonic belt (SSZ) in the eastern Indian Precambrian shield.

Acknowledgements—We thank A. Basu, D. S. Bhattacharyya, R. Chander, D. K. Mukhopadhyay, M. S. Pandian and V. N. Singh for reading the manuscript critically. Improvements suggested by R. J. Lisle, R. J. Norris, R. A. Glen and H. D. Ebert are acknowledged gratefully. Thanks are also due to P. L. Hancock for the comments on stress analysis and to Dhruba Mukhopadhyay for suggestions in Table 1.

REFERENCES

Anderson, E. M. 1951. *The Dynamics of Faulting*. Oliver and Boyd, Edinburgh.

Bahat, D. & Engelder, T. 1984. Surface morphology of transverse joints of the Appalachian plateau, New York and Pennsylvania. *Bull. geol. Soc. Am.* **104**, 299–313.

Berthé, D., Choukroune, P. & Jegouzo, P. 1979. Orthogneiss, mylonite, and non-coaxial deformation of granites: the example of south Armorican shear zone. *J. Struct. Geol.* **1**, 31–42.

Bhattacharyya D. S. & Sanyal, P. 1988. The Singhbhum Orogen—its structure and stratigraphy. In: *Precambrian of Eastern Indian Shield* (edited by Mukhopadhyay, D.). *Mem. geol. Soc. Ind.* **8**, 85–111.

Bieniawski, Z. T. 1967. Mechanics of brittle fracture of rock II. Experimental studies. *Int. J. Rock Mech. & Min. Sci.* **4**, 407–423.

Bose, M. K. & Chakraborty, M. K. 1981. Fossil marginal basin of the Indian shield: a model for the evolution of Singhbhum Precambrian belt. *Geol. Rdsch.* **70**, 504–518.

Choukroune, P., Gapais, D. & Merle, O. 1987. Shear criteria and structural symmetry. *J. Struct. Geol.* **9**, 525–530.

Coward, M. P. 1980. Shear zones in the Precambrian crust of South Africa. *J. Struct. Geol.* **2**, 19–27.

Dunn, J. A. 1929. Geology of north Singhbhum including parts of Manbhum district. *Mem. geol. Surv. Ind.* **54**, 1–66.

Dunn, J. A. & Dey, A. K. 1942. The geology and petrology of eastern Singhbhum and surrounding areas. *Mem. geol. Surv. Ind.* **69**, 281–452.

Durney, D. W. & Ramsay, J. G. 1972. Incremental strains measured by syntectonic crystal growths. In: *Gravity and Tectonics* (edited by De Jong, K. A. & Scholten, R.). John Wiley & Sons, New York, 67–92.

Eeckhout, B. & Zwart, H. J. 1988. Hercynian crustal scale shear zones in the Pyrenees. *Geology* **16**, 135–138.

Ghosh, S. & Sengupta, S. 1987. Progressive development of structures in ductile shear zones. *J. Struct. Geol.* **9**, 277–287.

Ghosh, S. & Sengupta, S. 1990. Singhbhum Shear Zone: Structural transition and kinematic model. *Proc. Ind. Acad. of Sci., Earth & Planet. Sci.* **99**, 229–247.

Grocott, J. 1977. The relationship between Precambrian shear belts and modern fault systems. *J. Geol. Soc. Lond.* **133**, 257–262.

Gupta, A., Basu, A. & Ghosh, P. K. 1980. The Proterozoic ultramafic and mafic lavas and tuffs of Dalma greenstone belt, Singhbhum, Bihar. *Can. J. Earth Sci.* **17**, 210–231.

Hancock, P. L. 1986. Joint spectra. In: *Geology in Real World, The Kingsley Dunham Volume* (edited by Nicol, I. & Nesbitt, R. W.). Institute of Mining and Metallurgy, London, 155–164.

Kulander, B. R. & Dean, S. L. 1985. Hackle plume geometry and joint propagation dynamics. In: *International Symposium on Fundamentals of Rock Joints*. Proceedings, 85–94.

McCourt, S. & Vearncombe, J. R. 1987. Shear zones bounding the central zone of Limpopo mobile belt, Southern Africa. *J. Struct. Geol.* **9**, 127–137.

Mukhopadhyay, D. 1976. Precambrian stratigraphy of Singhbhum—The problems and prospects. *Ind. J. Earth Sci.* **3**, 208–219.

Mukhopadhyay, D. 1990. Precambrian plate tectonics in the eastern Indian shield. In: *Crustal Evolution and Orogeny* (edited by Sychanthavong, S. P.). Oxford and IBH Publ. Co., 75–100.

Mukhopadhyay, D., Dasgupta, S. & Dhar, K. 1980. Basement slices within cover sediments near Hakegora and Jaikan, south of Tatanagar, Singhbhum district, Bihar. *J. Geol. Soc. Ind.* **21**, 286–294.

Mukhopadhyay, D., Ghosh, A. K. & Bhattacharyya, S. 1975. A reassessment of the structures of the Singhbhum Shear Zone. *Bull. Min. Metall. & Geol. Soc. Ind.* **48**, 49–67.

Nicolas, A., Bouchez, J. L., Blaise, J. & Poirier, J. P. 1977. Geological aspects of deformation in continental shear zones. *Tectonophysics* **42**, 55–73.

Park, R. J. 1981. Shear zone deformation and bulk strain in granite–greenstone terrane of the western Superior Province, Canada. *Precambrian Res.* **14**, 31–47.

Ramsay, J. G. 1967. *Folding and Fracturing of Rocks*. McGraw-Hill, New York.

Ramsay, J. G. & Graham, R. H. 1970. Strain variation in shear belts. *Can. J. Earth Sci.* **7**, 786–813.

Ramsay, J. G. & Huber, M. I. 1983. *The Techniques of Modern Structural Geology, Vol. I: Strain Analysis*. Academic Press, London.

Saha A. K., Ray, S. L. & Sarkar, S. N. 1988. Early history of the earth: Evidence from the eastern Indian shield. In: *Precambrian of the Eastern Indian Shield* (edited by Mukhopadhyay, D.). *Mem. Geol. Soc. Ind.* **8**, 13–38.

Saha A. K., Sarkar, S. N. & Ray, S. L. 1986. Importance of multiple method of dating in Precambrian Geology: examples from Singhbhum–Orissa region, Eastern India. *Ind. J. Earth Sci.* **13**, 129–144.

Sarkar, A. N. 1982. Precambrian tectonic evolution of eastern India: a model of converging microplates. *Tectonophysics* **86**, 363–397.

Sarkar, S. C., Gupta, A. & Basu, A. 1992. North Singhbhum Proterozoic mobile belt, Eastern India: Its character, evolution and metallogeny. In: *Metallogeny Related to Tectonics of Proterozoic Mobile Belts* (edited by Sarkar, S. C.). Oxford and IBH Publ. Co. New Delhi, 271–305.

Sarkar, S. N. & Saha, A. K. 1962. A revision of Precambrian stratigraphy and tectonics of Singhbhum and adjacent regions. *Quart. J. Min. Metall. & Geol. Soc. Ind.* **34**, 97–136.

Sarkar, S. N. & Saha, A. K. 1977. The present status of the Precambrian stratigraphy, tectonics and geochronology of the Singhbhum–Keonjhar–Mayurbhanj region, Eastern India. *Ind. J. Earth Sci.* (S. Ray Volume), 37–66.

Sarkar, S. N. & Saha, A. K. 1983. Structure and Tectonics of Singhbhum-Orissa Iron Ore craton. In: *Structure and Tectonics of Precambrian Rocks*, Recent Researches in Geology (edited by Sinha Roy, S.). Hindusthan Publishing Co., New Delhi, 1–25.

Sarkar, S. N., Saha, A. K. & Miller, J. A. 1969. Geochronology of the Precambrian rocks of Singhbhum and adjacent regions, Eastern India. *Geol. Mag.* **106**, 15–45.

Sarkar, S. N. & Srivastava, D. C. 1982. Structural analysis of the Archaean Iron Ore Group rocks south of copper belt shear zone in Chakradharpur–Ongarbira area, Singhbhum district, Bihar. *Ind. J. Earth Sci.* **9**, 116–130.

Srivastava, D. C. & Sarkar, S. N. 1985. Multiple deformation and interference structures in the Archaean Iron Ore Group rocks around Barda–Uluguta area, Singhbhum district, Bihar. *J. Geol. Soc. Ind.* **26**, 453–464.